





GREEN SYNTHESIS OF SILVER NANOPARTICLES USING *GALIUM VERUM* L. AQUEOUS EXTRACT AND EVALUATION OF ITS ANTIMICROBIAL ACTIVITY

Adriana-Maria ANDREICA^{a,*} , Mihaela Cecilia VLASSA^a ,
Rahela CARPA^b , Ioan PETEAN^c 

ABSTRACT. The development of cost-efficient and sustainable methods for the synthesis of nanomaterials still remains a scientific challenge. The aim of this study was to investigate the green synthesis of silver nanoparticles using aqueous extract of *Galium verum* L. (GV) as a potential source of biomolecules able to reduce the silver ions and stabilize them. Reaction parameters such as concentrations of AgNO₃, extract to AgNO₃ ratio, temperature, pH, and reaction time were optimized. The synthesis of silver nanoparticles (GV-AgNPs) using different parameters was monitored by ultraviolet-visible spectroscopy (UV-Vis). Fourier transform infrared spectroscopy (FTIR) results showed the presence of functional groups that act as reducing agents and stabilize the GV-AgNPs. Atomic force microscopy (AFM) confirmed that the particles were round-shaped with a diameter of about 25 nm. The GV-AgNPs show different antimicrobial activity depending on the type of sample and depending on the microbial strain tested.

Keywords: *green synthesis, nanoparticles, galium verum, antimicrobial activity*

INTRODUCTION

The production techniques of metallic nanoparticles and their applications made nanotechnology one of the most studied fields in the last decades [1, 2]. Metal nanoparticles have attracted considerable attention due to their diverse

^a Babeş-Bolyai University, "Raluca-Ripan" Institute for Research in Chemistry, 30 Fântânele str., RO-400294, Cluj-Napoca, Romania

^b Babeş-Bolyai University, Faculty of Biology and Geology, Molecular Biology and Biotechnology Department, 1 Mihail Kogălniceanu str., RO-400084, Cluj-Napoca, Romania

^c Babeş-Bolyai University, Faculty of Chemistry and Chemical Engineering, 11 Arany Janos str., RO-400084, Cluj-Napoca, Romania

* Corresponding author: adriana.andreica@ubbcluj.ro



applications in different fields such as biomedicine (fast diagnosis, imaging, tissue regeneration drug delivery, and development of new medical products) [3], catalysis [4], and electronics [5]. Generally, the synthesis of silver nanoparticles is carried out using physicochemical techniques such as autoclaving [6], gamma-ray radiation [7], and use of microemulsions [8], electrochemical techniques [9], chemical reduction [10], laser ablation [11], microwave irradiation [12], and photochemical reduction [13]. The synthesis has limitations such as the use of toxic chemicals and generation of hazardous waste, high functional cost, and energy requirement. Green nanotechnology has been developed as an alternative to the use of environmentally harmful processes and products [14]. Plant extracts can be used to obtain silver nanoparticles without the need for harmful reducing and capping chemicals, and high temperatures. The use of plant extracts for the synthesis of silver nanoparticles provides a low-cost, non-toxic, environmentally friendly method. There are several studies that report the synthesis of silver nanoparticles by exploiting the reducing capacity of flavonoids, phenolics, proteins, and carbohydrates from plants with pharmacological properties [15, 16].

Galium verum L., also known as Lady's Bedstraw, belonging to the Rubiaceae family, is a perennial herb widely used throughout history in traditional medicine as diuretic, choleric and treatment for gout and epilepsy [17]. *Galium verum* L. extracts are known to have antimicrobial and antioxidant properties [18, 19], improve *in vivo* cardiac function in rats, preserve the functional and morphological properties of the heart, and prevent coronary dysfunction after ischemia [20], and reveal a growth-inhibiting effect on chemo-sensitive and -resistant laryngeal carcinoma cell lines [21]. *Galium verum* L. extracts have been studied for their chemical composition, a variety of bioactive substances have been identified, such as iridoid glycosides [22], flavonoids [23, 24], and phenolic acids [25, 24].

Beyond the use of this plant for medicinal purposes and taking into account its chemical composition, *Galium verum* L. extract was chosen for the synthesis of silver nanoparticles.

The novelty of this study was the use for the first time of *Galium verum* L. extract as a source of biomolecules that can act as a reducing agent and stabilizer in the synthesis of silver nanoparticles in a highly sustainable manner and the testing of the antimicrobial activity of the obtained nanoparticles. The aim of the present study was to investigate the green synthesis of silver nanoparticles using the aqueous extract of *Galium verum* L. aerial parts, to optimize the reaction parameters, to characterize the obtained nanoparticles, and to evaluate their antimicrobial activity against Gram-positive, Gram-negative strains and fungal strain. To the best of our knowledge, the synthesis of GV-AgNPs and their antimicrobial activity have not been previously reported.

RESULTS AND DISCUSSION

To obtain GV-AgNPs, different parameters were evaluated, namely, silver salt concentration, temperature, volume ratio of plant extract to silver salt solution, pH value of the solution, and reaction time. The formation of silver nanoparticles was monitored by UV-Vis spectroscopy, which is the main tool used to study the synthesis. The formation of silver nanoparticles was first visually observed by the color change from yellow to dark brown due to the excitation of surface plasmon resonance (SPR) of the nanoparticles [26]. The reduction of silver ions using GV extract was confirmed by the UV-Vis spectrum, which showed a characteristic surface plasmon resonance peak at 411 nm, which was in agreement with the literature data [27]. This peak provides information on the morphology of the obtained silver nanoparticles.

The absorption peak of the GV-AgNPs was broad and less intense when the concentration of AgNO_3 was 1 mM, as shown in Figure 1 (A), which indicates that silver nanoparticles were agglomerated. By increasing the concentration of AgNO_3 , an increase in the intensity of the peak was observed. The absorption peak was 409 nm and became sharper. This suggests that obtained GV-AgNPs were relatively smaller as the AgNO_3 concentration increased to 10 mM. In Figure 1 (B) the effect of temperature variation on silver nanoparticle synthesis is presented. By increasing the temperature, the absorption peak was shifted from 421 nm at 30 °C and 424 nm at 50 °C to 409 nm at 70 °C. The disappearance of broadening and an increase in intensity of the absorption peak were also observed. The broad and shifted peak to longer wavelengths was attributed to agglomeration or an increase in size of the nanoparticles [28, 29].

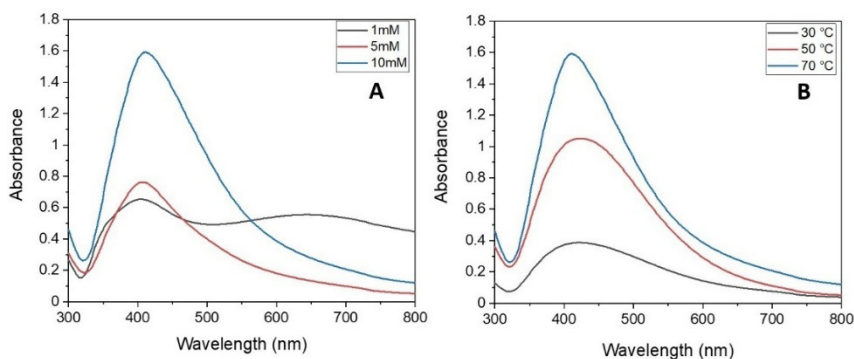


Figure 1. UV-Vis spectra: Effect of concentration and temperature on silver nanoparticles synthesis: (A) different concentrations of AgNO_3 , extract to AgNO_3 ratio = 1:20, $T = 70$ °C, $\text{pH} = 8$, reaction time = 4 h; (B) 10 mM AgNO_3 , extract to AgNO_3 ratio = 1:20, $\text{pH} = 8$ at different temperatures

The absorption peak of the GV-AgNPs was broad and less intense when extract to AgNO₃ volume ratios used in synthesis were 1:5 and 1:10, as shown in Figure 2 (C). The GV-AgNPs obtained with a 1:20 ratio between extract and AgNO₃ showed a strong and sharp absorption peak at 411 nm.

Based on other studies that confirm that an alkaline medium was favorable for the silver nanoparticles [30], pH = 8 was chosen to obtain GV-AgNPs, but the synthesis was also tested at pH 6 and pH 10, as illustrated in Figure 2 (D). By increasing the pH value of the reaction media, the absorption peak was shifted from 429 nm at pH = 6 to 411 nm at pH = 8 and 414 nm at pH = 10. The obtained silver nanoparticles at pH = 8 were smaller, and the absorption peak was sharp. The absorption peak shifts towards shorter wavelengths when the size of nanoparticles decreases [29], and an increase in the intensity peak means an increase in the concentration of nanoparticles [31].

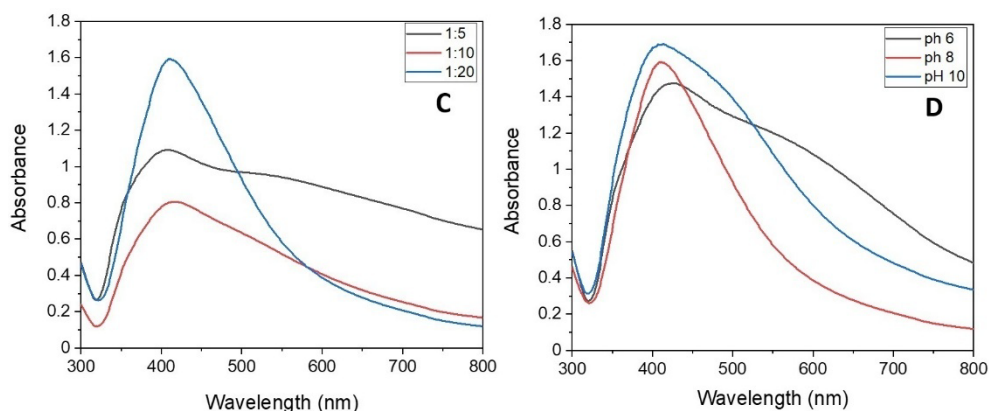


Figure 2. UV-Vis spectra: Effect of extract to AgNO₃ ratio and effect of pH on silver nanoparticles synthesis: (C) different extract to AgNO₃ ratio, 10 mM AgNO₃, pH = 8, T = 70 °C, reaction time = 4 h; (D) extract to AgNO₃ ratio = 1:20, 10 mM AgNO₃, T = 70 °C, reaction time = 4 h at different pH values

The effect of the reaction time on GV-AgNPs synthesis is presented in Figure 3.

The intensity of the absorption peak increased after 4 hours, indicating an increase in the concentration of silver nanoparticles with time [32], while at 6 hours the intensity of the absorption peak decreased.

The optimum parameters for the green synthesis of GV-AgNPs were AgNO₃ concentration 10 mM, 1:20 volume ratio of *Galium verum* L. extract to AgNO₃, pH 8, temperature 70 °C and reaction time 4 h.

GREEN SYNTHESIS OF SILVER NANOPARTICLES USING *GALIUM VERUM* L. AQUEOUS EXTRACT AND EVALUATION OF ITS ANTIMICROBIAL ACTIVITY

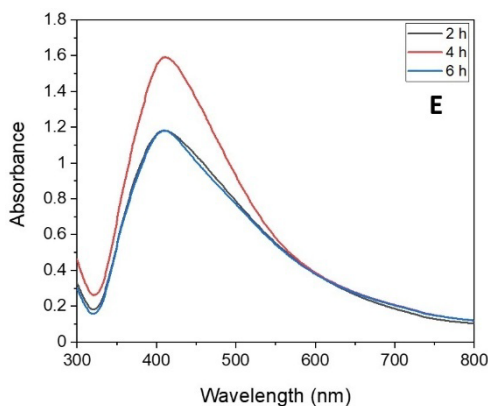


Figure 3. UV-Vis spectra: Effect of reaction time on silver nanoparticles synthesis: (E) 10 mM AgNO₃, extract to AgNO₃ ratio = 1:20, pH = 8, T = 70 °C

Fourier transformed infrared spectroscopy was used to identify the organic molecules from the aerial parts extract of the plant that act as reducing agents of the silver ions and stabilize the obtained silver nanoparticles. The FTIR spectra of *Galium verum* L. aqueous extract and silver nanoparticles obtained by the green synthesis are shown in Figure 4.

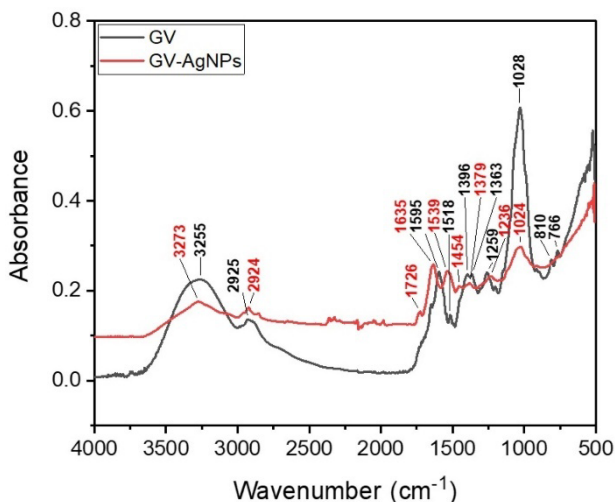


Figure 4. FTIR spectra for *Galium verum* L. extract and silver nanoparticles

The results of the FTIR analysis for both *Galium verum* L. extract and silver nanoparticles (GV-AgNPs) are presented in Table 1. The assignment of stretching and bending vibrations was carried out in accordance with the literature data.

Table 1. FTIR absorption bands assignment of *Galium verum* L. extract and obtained silver nanoparticles

Wavenumber (cm ⁻¹)		Assignment	Functional groups	References
GV	GV-AgNPs			
3255	3273	OH stretch	Alcohols/Phenols	[33]
2925	2924	CH stretching/ OH stretch	Alkanes/Alcohols (acid)	[34, 35]
	1726	C=O stretch	Carbonyl compounds	[35]
1595	1635	C=O and C=C stretching	Unsaturated Ketones	[35, 36, 37]
1518	1539	C=C stretch	Aromatic compounds	[38, 34]
	1454	CH bending/ C=C stretch	Alkanes/Aromatic compounds	[34, 35]
1396		CH bending	Alkanes	[35]
1363	1379	CH bending	Alkanes	[34]
1259	1236	C-O-C stretch	Ethers/Esters	[33, 35]
1028	1024	C-O stretch	Alcohols	[36]
810		C=C bending/C-Cl stretching	Alkanes/Halo compounds	[34]
766		C=C bending/C-Cl stretching	Alkanes/Halo compounds	[34]

In both the extract and GV-AgNPs FTIR spectra the presence of different functional groups that are involved in the synthesis and stabilization of silver nanoparticles was observed (Figure 4). In the *Galium verum* L. extract spectrum, the absorption band at 3255 cm⁻¹ was attributed to OH stretching vibrations of the phenols, and the band at 2925 cm⁻¹ was attributed to CH₂ asymmetric stretching vibrations or OH stretching in acid functional groups. The band at 1595 cm⁻¹ can be attributed to C=O and C=C stretching vibrations in α , β -unsaturated ketones. The absorption peaks between 1300 and 1600 cm⁻¹ show the presence of C=C stretch in a ring and CH bending from aromatic compounds and alkanes (CH₂ and CH₃ bending). The bands at 1259 cm⁻¹ were attributed to C-O-C stretch in ethers and esters, and the sharp one at 1028 cm⁻¹ to C-O stretch in alcohols. The bands at 810 cm⁻¹ and 766 cm⁻¹ were assigned to C=C bending vibrations in alkanes and C-Cl stretching in halo compounds. The FTIR spectrum of the extract was compared with the GV-AgNPs spectrum. Some shifts were observed as follows: OH, C=O and C=C, C=C, CH, C-O-C, C-O groups were shifted from 3255, 1595, 1518, 1363, 1259 and 1028 cm⁻¹ to 3273, 1635, 1539, 1379, 1236 and 1024 cm⁻¹. It was observed that nanoparticles showed a new band at 1726 cm⁻¹

GREEN SYNTHESIS OF SILVER NANOPARTICLES USING *GALIUM VERUM* L. AQUEOUS EXTRACT AND EVALUATION OF ITS ANTIMICROBIAL ACTIVITY

corresponding to carbonyl stretching vibrations in aldehydes or ketones. The stretching bands related to the carbonyl groups at 1635 cm^{-1} and 1726 cm^{-1} may be indicating the involvement of hydroxyl groups in the reduction of Ag^+ to Ag^0 resulting in oxidized polyphenols that act as capping agents and stabilize the formed silver nanoparticles [39, 40]. *Galium verum* L. extracts contain phenolic acids such as chlorogenic acid, caffeic acid, ferulic acid, coumaric acid, and flavonoids [41-43]. Many studies have mentioned the role of polyphenols from plant extracts in the green synthesis of silver nanoparticles that can reduce and stabilize them [44-47].

The atomic force microscopy (AFM) was used for the topographic characterization of the self assembled GV-AgNPs onto solid substrate. The general aspect of the formed thin film is uniform and smooth, indicating a uniform adsorption of the nanoparticles from the liquid dispersion, Figure 5a.

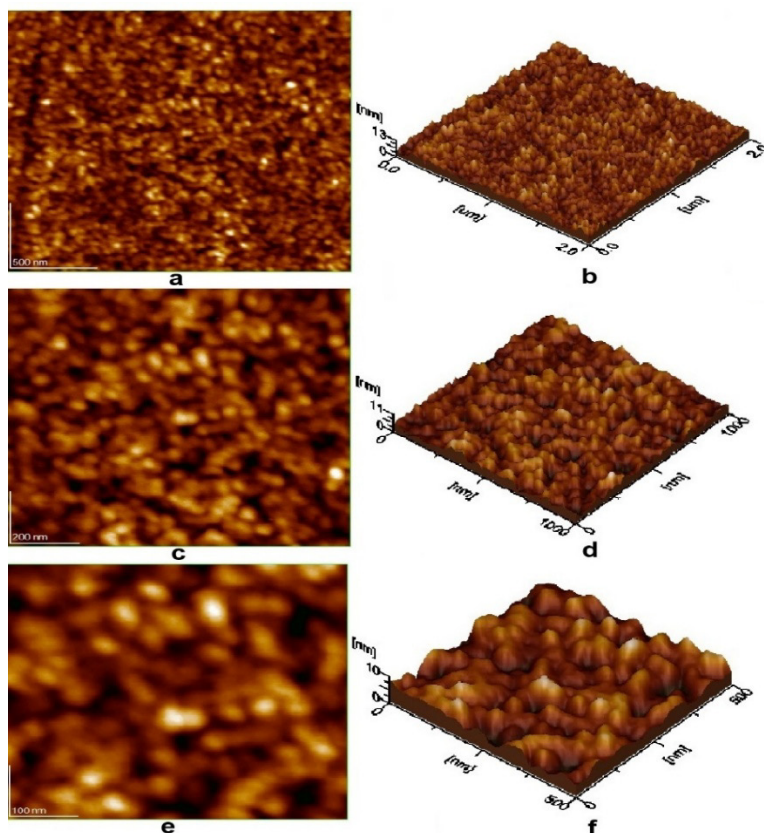


Figure 5. AFM images of synthesized GV-AgNPs; scanned area $2\ \mu\text{m} \times 2\ \mu\text{m}$; $1\ \mu\text{m} \times 1\ \mu\text{m}$; $0.5\ \mu\text{m} \times 0.5\ \mu\text{m}$: (a, c, e) 2D-topography; (b, d, f) three-dimensional profiles

It ensures a low surface roughness of 1.61 ± 0.28 nm, which is well correlated with the flat aspect of the three-dimensional profile presented in Figure 5b. A closer look to the self assembled structure can be observed at the scanned area of $1 \mu\text{m} \times 1 \mu\text{m}$ in Figure 5c. The nanoparticles appear well individualized without marginal coalescence, allowing observation of their rounded shape. The lack of submicron clusters, which would have been formed at a high coalescence gradient, indicates an increased efficiency of the nanoparticles to hit and penetrate the membranes of the pathogen agent causing their death.

The three-dimensional profile in Figure 5d reveals the nanoparticles deposition mode on specific areas of the targeted microorganism surface. The local roughness is situated around 1.62 ± 0.16 nm, it is significantly low as a thin film but its efficacy must to be proved by the antimicrobial testing results.

The nanostructural detail taken at the scanned area of $0.5 \mu\text{m} \times 0.5 \mu\text{m}$, Figure 5e, allows the proper measuring of the nanoparticles diameter, which is about 25 ± 3 nm.

The silver nanoparticles obtained by the use of *Majorana hortensis* extract were characterized by AFM, and the size of nanoparticles was in the range of 50 and 95 nm [48]. The literature data show that 25 nm is an ideal diameter for antibacterial purposes [15, 16]. The perfect individualization of the adsorbed nanoparticles is observed better in the three-dimensional profile in Figure 5e, revealing their adhesion mode on the pathogen cell membrane.

Evaluation of antimicrobial activity

After the end of the incubation period at 37°C , the zones of inhibition (mm) for the tested microbial strains were determined. It was observed that in all bacterial strains, the control sample CN10 (gentamicin) showed inhibition between 12 and 22 mm. For the *Candida albicans* strain, the control sample VOR1 (voriconazole) showed a stronger inhibition of 28 mm (Figure 6, Figure 7). The *Galium verum* extract showed a slight inhibition compared to the chosen control (CN10 for bacterial strains and VOR1 for fungal strain). However, *Galium verum* species can be used as a good source of polyphenols with antibacterial properties.

The diameter of the inhibition zone in microbial strains after the incubation period is presented in Figure 7.

For Gram positive bacterial strains, different diameters of inhibition were recorded. At *Staphylococcus aureus* ATCC 25923, inhibition was noticed only at the sample with GV-AgNPs (12 mm). At *Enterococcus faecalis* ATCC 29212, both samples showed inhibition, but the GV extract sample showed higher inhibition (15 mm) than the GV-AgNPs sample.

GREEN SYNTHESIS OF SILVER NANOPARTICLES USING *GALIUM VERUM* L. AQUEOUS EXTRACT AND EVALUATION OF ITS ANTIMICROBIAL ACTIVITY

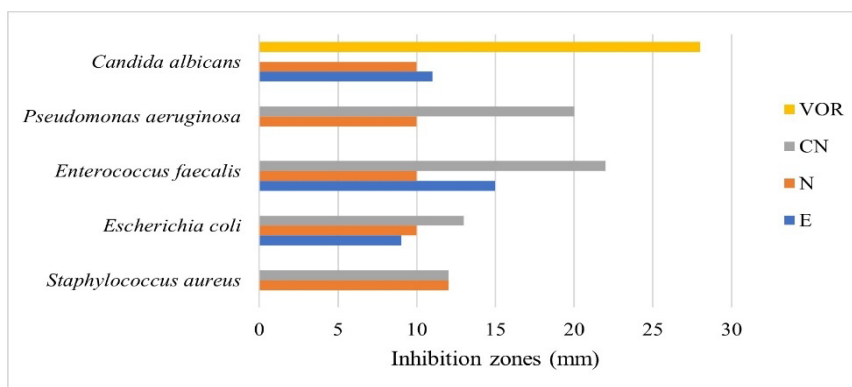


Figure 6. The diameter of the inhibition zones (mm) of the tested samples (E = GV extract, N = GV-AgNPs, CN = gentamicin, VOR = voriconazole)

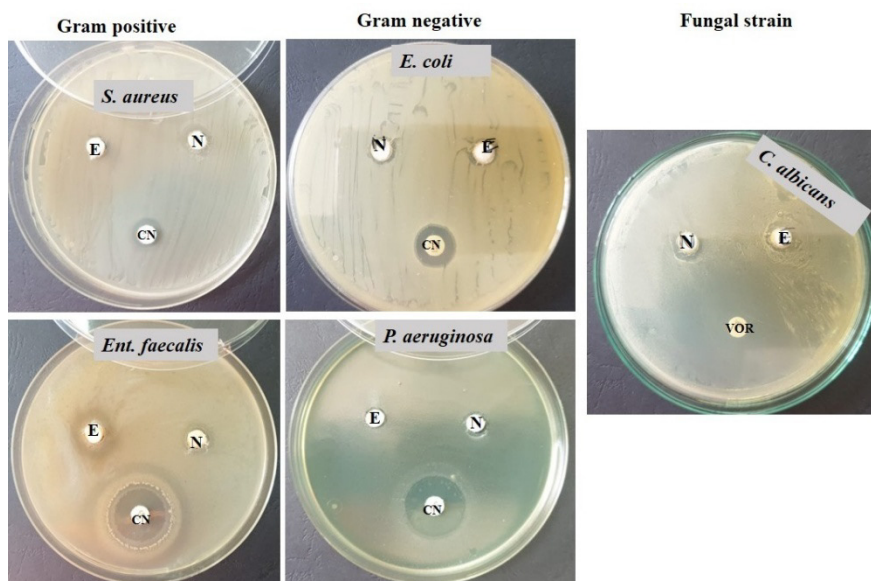


Figure 7. The diameter of the inhibition zone in microbial strains after the incubation period (E = GV extract, N = GV-AgNPs, CN = gentamicin, VOR = voriconazole)

For Gram negative bacterial strains, different inhibition diameters were recorded. At *Escherichia coli* ATCC 25922, both samples showed slight inhibition. In the *Pseudomonas aeruginosa* ATCC 27853 strain, only the sample with GV-AgNPs showed a slight inhibition (10 mm). It was observed that the Gram negative strains tested showed less inhibition than the Gram positive ones.

In the fungal strain *Candida albicans* ATCC 10231, the tested samples showed a slight inhibition (sample E = 10 mm and sample N = 11 mm) compared to the control sample (VOR), which recorded an inhibition of 28 mm.

CONCLUSIONS

The present study reports the green synthesis of silver nanoparticles using *Galium verum* L. extract as a source of biomolecules capable of the reduction and stabilization of the nanoparticles obtained. By optimizing the reaction parameters and using sustainable raw materials such as *Galium verum* L. extract, this process provides an easy way to obtain silver nanoparticles. UV-Vis spectroscopy was used to confirm the presence of the characteristic SPR peak at 411 nm, indicating the synthesis of GV-AgNPs. The presence of functional groups involved in the synthesis and stabilization of the GV-AgNPs was identified by FTIR spectroscopy. The topographic characterization of the GV-AgNPs by AFM indicated well individualized nanoparticles of rounded shape and with a diameter of about 25 nm.

The self assembly of the GV-AgNPs onto the solid surface indicates an efficient mode of targeting the membrane of the pathogen agent facilitating their antibacterial action.

The antimicrobial activity of GV-AgNPs was evaluated using an antimicrobial diffusion test on Gram positive, Gram negative bacterial strains, and fungal strain. Following these experiments on *Galium verum* L. extract and GV-AgNPs it can be stated that they show different antimicrobial activity depending on the type of sample and depending on the microbial strain tested.

The synthesis of GV-AgNPs by the green process is a promising tool for new research strategies due to its potential for various medical applications.

EXPERIMENTAL SECTION

Materials

The aerial parts of *Galium verum* L. were collected in June 2024 during the flowering period from Florești, Cluj County, România. The plant was identified at the “Alexandru Borza” Botanical Garden from Cluj-Napoca, and the voucher specimen (no. 674506) was deposited in the CL Herbarium Musei Universitatis Napocensis, Cluj-Napoca. Silver nitrate (AgNO_3) was purchased from Merck România and was of analytical grade. Ultrapure water (18.2 M Ω cm ionic purity at 25 °C) produced in the laboratory by means of a Simplicity system (Millipore; Bedford, MA, USA) was used in all experiments.

Preparation of aqueous extract

Aerial parts of the collected plant were washed with running tap water and dried in the shade at room temperature. The dried plant was ground to powder. 100 mL of ultrapure water was added to 10 g of plant powder and boiled for 20 minutes. The cooled extract was filtered with Whatman filter paper no. 1 and stored at 4 °C until further use.

Green synthesis of silver nanoparticles

For the synthesis of silver nanoparticles, 2.5 mL of plant extract was added to a 50 mL silver nitrate solution of different concentrations (1 mM, 5 mM, 10 mM). The reactions were effectuated at 30, 50, 70 °C. The volume ratios of extract to silver nitrate solution used in nanoparticle preparation were 1:5, 1:10, and 1:20. Different pH values (6, 8, 10) were investigated. The reaction was monitored by UV-Vis spectroscopy at 2 h, 4 h, and 6 h.

The best results were obtained as follows: extract (2.5 mL) was added to a 10 mM AgNO₃ solution (50 mL) using a 1:20 volume ratio of extract to AgNO₃ solution, and then pH of the reaction mixture was adjusted to 8 using a 0.1 M NaOH solution. After 4 hours of stirring at 70 °C, the obtained nanoparticles were purified by centrifugation for 20 minutes, washed three times with ultrapure water, and then lyophilized.

Characterization of the GV-AgNPs

The synthesis of AgNPs was monitored by UV-Vis spectroscopy using a Specord 205 Spectrophotometer (Analytik Jena, GmbH, Germany). The sample was diluted with ultrapure water, and then the UV-Vis spectra were recorded using ultrapure water as the blank. The identification of functional groups involved in both plant extract and silver nanoparticles was performed by Fourier transform infrared spectroscopy (FTIR) using FTIR 610 spectrometer (Jasco Corporation, Tokyo, Japan), equipped with an ATR attachment (attenuated total reflectance) with a horizontal ZnSe crystal (Jasco PRO400S) in the 4000-500 cm⁻¹ wave number range. The resolution of the spectra was 4 cm⁻¹ and scans were repeated of 100 times. All FTIR spectra were registered at room temperature.

The nanoparticles were transferred onto a solid substrate (e.g. a glass slide) by vertical adsorption for 20 seconds, followed by natural drying. Nanoparticles aspect and their self-assembly ability on solid substrate were investigated with Atomic Force Microscopy (AFM). It was effectuated with a JEOL JSPM 4210 Scanning Probe Microscope operated in tapping mode using NSC 15 Hard cantilever with a resonant frequency of 325 kHz and

a force constant of 40 N/m. The nanoparticles size and surface roughness were measured with specific software, WinSPM 2.0 produced by Jeol Company, Japan, according to the procedures previously described in literature [49, 50].

Antimicrobial activity evaluation of the GV-AgNPs

Antimicrobial diffusion test. *Staphylococcus aureus* ATCC 25923, *Escherichia coli* ATCC 25922, *Pseudomonas aeruginosa* ATCC 27853, *Enterococcus faecalis* ATCC 29212 and *Candida albicans* ATCC 10231 from Microbiology Lab (Faculty of Biology and Geology, UBB, Cluj-Napoca) were used in this research. Bacterial strains were cultivated on Nutrient Agar, while *Candida* was grown on Sabouraud Agar medium [51]. Then the bacterial culture was suspended in saline on 0.5 McFarland turbidity, and it was swabbed uniformly across an agar plate (Mueller Hinton-Oxoid).

The plates were dried for 15 minutes at 37 °C. For the samples to be tested, wells were made in the culture medium with sterile tips of 5 mm diameter. Then, in these wells, sterile cotton swabs were placed. Out of the tested samples (E = GV-extract, N = GV-AgNPs) 100 µL were placed in each well. CN10 = gentamicin (for bacterial strains) and VOR1 = voriconazole (for *Candida* strain) were used as control. The incubation time was 48 hours at 37 °C. The reading was made by measuring the diameter of the zone of inhibition that appeared around the well with the sample on the culture medium: the larger the diameter of the zone of inhibition, the greater the sensitivity of the bacteria to the respective antibacterial substances [52].

ACKNOWLEDGMENTS

The authors thank to dr. I. L. Szigyarto and dr. M. Puşcaş for *Galium verum* L. identification.

REFERENCES

1. K. K. Harish; N. Venkatesh; H. Bhowmik; A. Kuila; *Biomed. J. Sci. Tech. Res.*, **2018**, 4, 3765-3775
2. S. Padalkar; J. R. Capadona; S. J. Rowan; C. Weder; Y. H. Won; L. A. Stanciu; R. J. Moon; *Langmuir*, **2010**, 26, 8497-8502
3. K. S. B. Naidu; P. Govender; J. K. Adam; *J. Pure Appl. Microbiol.*, **2015**, 9, 103-112
4. X. Y. Dong; Z. W. Gao; K. F. Yang; W. Q. Zhang; L. W. Xu; *Catal. Sci. Technol.*, **2015**, 5, 2554–2574

5. R. Abbas; J. Luo; X. Qi; A. Naz; I. A. Khan; H. Liu; S. Yu; J. Wei; *Nanomaterials*, **2024**, *14*, 1425
6. A. Jamaludin; C. K. Faizal; *Indian J. Sci. Technol.*, **2017**, *10*, 1-5
7. P. Chen; L. Song; Y. Liu; Y. E. Fang; *Radiat. Phys. Chem.*, **2007**, *76*, 1165–1168
8. M. Andersson; J. S. Pedersen; A. E. C. Palmqvist; *Langmuir*, **2005**, *21*, 11387–11396
9. R. A. Khaydarov; R. R. Khaydarov; O. Gapurova; Y. Estrin; T. Scheper; *J. Nanopart. Res.*, **2009**, *11*, 1193–1200
10. H. Wang; X. Qiao; J. Chen; S. Ding; *Colloids Surf. A: Physicochem. Eng. Asp.*, **2005**, *256*, 111–115
11. A. Pyatenko; K. Shimokawa; M. Yamaguchi; O. Nishimura; M. Suzuki; *Appl. Phys. A.*, **2004**, *79*, 803–80
12. A. Pal; S. Shah; S. Devi; *Mater. Chem. Phys.*, **2009**, *114*, 530–532
13. R. F. Elsupikhe; M. B. Ahmad; K. Shameli; N. A. Ibrahi; N. Zainuddin; *IEEE Trans. Nanotechnol.*, **2016**, *15*, 209–213
14. P. Khandel, P; R. K. Yadav; D. K. Soni; L. Kanwar; S. K. Shahi; *J. Nanostruct. Chem.*, **2018**, *8*, 217-254
15. S. C. Jain; M. S. Mehata; *Sci. Rep.*, **2017**, *7*, 15867
16. L. Wang; Y. Wu; J. Xie; S. Wu; Z. Wu; *Mater. Sci. Eng. C.*, **2018**, *86*, 1-8
17. J. Bradic; A. Petkovic; M. Tomović; *Serb. J. Exp. Clin. Res.*, **2018**, *22*, 187-193
18. I. T. Vasilevna; G. O. Volodymyrivna; T. E. Leonidivna; K. I. Aleksandrovna; K. A. Mihaylovna; *Pharmacogn. Commn.*, **2016**, *6*, 42-47
19. P. -R. Laanet; P. Saar-Reismaa; P. Jõul; O. Bragina; M. Vaher; *Molecules*, **2023**, *28*, 2867
20. J. Bradic; V. Zivkovic; I. Srejovic; V. Jakovljevic; A. Petkovic; T. N. Turnic; J. Jeremic; N. Jeremic; S. Mitrovic; T. Sobot; N. Ponorac; M. Ravic; M. Tomovic; *Oxid. Med. Cell. Longev.*, **2019**, 4235405
21. M. Schmidt; C. J. Scholz; G. L. Gavril; C. Otto; C. Polednik; J. Roller; R. Hagen; *Int. J. Oncol.*, **2014**, *44*, 745-760
22. L. Ö. Demirezer; F. Gürbüz; Z. Güvenalp; K. Ströch; A. Zeeck; *Turk. J. Chem.*, **2006**, *30*, 525-534
23. C. C. Zhao; J. H. Shao; X. Li; X. D. Kang; Y. W. Zhang; D. L. Meng; N. Li; *J. Asian Nat. Prod. Res.*, **2008**, *10*, 611-615
24. A. D. Farcas; A. C. Mot; C. Zagrean-Tuza; V. Toma; C. Cimpoi; A. Hosu; M. Parvu; I. Roman; R. Silaghi-Dumitrescu; *PLoS One*, **2018**, *13*, e0200022
25. L. Vlase; A. Mocan; D. Hanganu; D. Benedec; A. Gheldiu; G. Crişan; *Digest J. Nanomater. Biostruct.*, **2014**, *9*, 1085-1094
26. P. Mulvaney; *Langmuir*, **1996**, *12*, 788–80
27. C. Ozdemir; M. Gencer; I. Coksu; T. Ozbek; S. Derman; *Arh. Hig. Rada Toksikol*, **2023**, *74*, 90-98
28. M. Ndikau; N. M. Noah; D. M. Andala; E. Masika; *Int. J. Anal. Chem.*, **2017**, 8108504
29. S. Ansar; H. Tabassum; N. S. M. Aladwan; M. N. Ali; B. Almaarik; S. AlMahrouqi; M. Abudawood; N. Banu; R. Alsubki; *Sci. Rep.*, **2020**, *10*, 18564
30. M. Vanaja; S. Rajeshkumar; K. Paulkumar; G. Gnanajobitha; C. Malarkodi; G. Annadurai; *Adv. Appl. Sci. Res.*, **2013**, *4*, 50-55

31. M. Sathishkumar; K. Sneha; Y. S. Yun; *Bioresour. Technol.*, **2010**, *101*, 7958-7965
32. S. Pugazhendhi; P. Sathya; P. K. Palanisamy; R. Gopalakrishnan; *J. Photochem. Photobiol. B*, **2016**, *159*, 155-160
33. S. Khan; S. Shujah; U. Nishan; S. Afridi; M. Asad; A. U. H. A. Shah; N. Khan; S. Ramzan; M. Khan; *Arab. J. Sci. Eng.*, **2023**, *48*, 7673–7684
34. A. D. Semenescu; E. A. Moacă; A. Iftode; C. A. Dehelean; D. S. Tchiakpe-Antal; L. Vlase; A. M. Vlase; D. Muntean; R. Chioibaş; *Molecules*, **2023**, *28*, 7804
35. J. B. Lambert; H. F. Shurvell; R. G. Cooks; *Organic Structural Spectroscopy*, Prentice-Hall Inc., New Jersey, **1998**
36. N. H. Reza zadeh; F. Buazar; S. Matroodi; *Sci. Rep.*, **2020**, *10*, 19615
37. S. Narath; S. S. Shankar; S. K. Sivan; B. George; T. D. Thomas; S. Sabarinath; S. K. Jayaprakash; S. Waclawek; V. V.T. Padil; *Ecol. Chem. Eng. S.*, **2023**, *30*, 7-21
38. A. Deep; M. Verma; R. K. Marwaha; A. K. Sharma; B. Kumari; *Curr. Cancer Ther. Rev.*, **2019**, *15*, 1-7
39. K. M. Kumar; B. K. Mandal; H. A. K. Kumar; S. B. Maddinedi; *Spectrochim. Acta A Mol. Biomol. Spectrosc.*, **2013**, *116*, 539-545
40. A. J. Kora; S. R. Beedu; A. Jayaraman; *Org. Med. Chem. Lett.*, **2012**, *2*, 17
41. A. O. Danila; F. Gatea; G. L. Radu; *Chem. Nat. Compd.*, **2011**, *47*, 22–26
42. A. O. Matei; F. Gatea; G. L. Radu; *J. Chromatogr. Sci.*, **2015**, *53*, 1147–1154
43. A. Mocan; G. Crişan; L. Vlase; B. Ivănescu; A. S. Bădărău; A. L. Arsene; *Farmacia*, **2016**, *64*, 95-99
44. N. Swilam; K. A. Nemataallah; *Sci. Rep.*, **2020**, *10*, 14851
45. Q. Lin; H. Huang; L. Chen; G. Shi; *Biomed. Res.*, **2017**, *28*, 1276-1279
46. M. C. Lite; R. Constantinescu; E. C. Tănăsescu; A. Kuncser; C. Romaniţan; D. E. Mihaiescu; I. Lacatusu; N. Badea; *Materials*, **2023**, *16*, 3924
47. L. David; B. Moldovan; *Studia UBB Chemia, LXVII*, **2022**, *3*, 37-44
48. J. K. T. Al-Isawi; A. M. Mohammed; D. T. A. Al-Heetimi; *Studia UBB Chemia, LXVIII*, **2023**, *2*, 131-144
49. S. E. Avram; B. V. Birle; L. B. Tudoran; G. Borodi; I. Petean; *Water*, **2024**, *16*, 1027
50. S. E. Avram; L. B. Tudoran; S. Cuc; G. Borodi; B. V. Birle; I. Petean; *J. Compos. Sci.*, **2024**, *8*, 219
51. R. M. Atlas; *Handbook of Microbiological Media*, 4th ed., CRC Press, New York, **2010**
52. R. Carpa; M. Drăgan-Bularda; V. Muntean; *Microbiologie Generală Lucrări Practice (General Microbiology, Practical Works)*, Cluj University Press Publishing House, **2014**